

# The ( $^{18}\text{O},^{16}\text{O}$ ) reaction: a bridge from direct to dissipative dynamics

**M. Cavallaro<sup>1a</sup>, M. Colonna<sup>a</sup>, F. Cappuzzello<sup>a,b</sup>, C. Agodi<sup>a</sup>, M. Bondi<sup>a,b</sup>, D. Carbone<sup>a</sup>, A. Cunsolo<sup>a</sup>, M. De Napoli<sup>c</sup>, A. Foti<sup>b,c</sup>**

<sup>a</sup> INFN – LNS, Catania, Italy

<sup>b</sup> Dipartimento di Fisica e Astronomia, Università degli Studi di Catania, Catania, Italy

<sup>c</sup> INFN – Sezione di Catania, Catania, Italy

E-mail: manuela.cavallaro@lns.infn.it

**Abstract.** A study of the ( $^{18}\text{O},^{16}\text{O}$ ) two-neutron transfer reaction at 84 MeV incident energy was pursued at the Catania INFN-LNS laboratory on several targets. In the energy spectra obtained from the light targets, several known low lying and resonant states of the product nuclei are observed. Instead, the spectra from the heavier targets are dominated by the appearance of a broad bump, indicating that more dissipative processes are contributing. In this case, calculations based on semi-classical transport theories seem to indicate the possible occurrence of dissipative reaction mechanisms.

## 1. Introduction

Direct transfer reactions represent essential tools in nuclear physics since they have the basic property to select specific degrees of freedom in the complex many body nuclear system. For this reason, they have always played a crucial role in the investigation of the nuclear structure. For example, a subject of great interest is the connection between transfer probabilities in two-neutron transfer reactions and pairing correlations in nuclei [1], [2], [3].

In the past, spectroscopic investigations of single-particle as well as cluster configurations above the Fermi level were mainly conducted by light ions induced reactions. Moreover the potentiality of heavy-ion two-neutron transfer reactions has not been fully exploited till now [4], [5] also due to the experimental difficulties in producing high-resolution spectra covering a wide energy and angular range [6]. Nevertheless, studies with heavy projectiles demonstrate their reliability for quantitative analyses, as long as the multistep processes remain comparatively weak [7] or are explicitly accounted for.

An interesting case, which has been focused in a recent paper [1], is given by transfer reactions driven by  $^{18}\text{O}$  beam. In particular it turned out that spectroscopic factors can be

---

1 To whom any correspondence should be addressed.



extracted for both one- and two-neutron configurations, opening the door to future application of heavy-ion reactions as spectroscopic tools.

In this context, a systematic exploration of the response of atomic nuclei to the ( $^{18}\text{O},^{16}\text{O}$ ) and ( $^{18}\text{O},^{17}\text{O}$ ) probes has started at the INFN-LNS in Catania at bombarding energy slightly above the Coulomb barrier.

In the present manuscript a specific attention is paid to the  $^{64}\text{Ni}(^{18}\text{O},^{16}\text{O})^{66}\text{Ni}$  reaction, which shows hints for the evolution of the reaction mechanism from a pure direct to a more dissipative process.

## 2. The experiment

The  $^{64}\text{Ni}(^{18}\text{O},^{16}\text{O})^{66}\text{Ni}$  reaction was studied at the INFN-LNS laboratory in Catania. The  $^{18}\text{O}$  beam was delivered at 84 MeV total incident energy by the Tandem accelerator. The experiment was performed on a  $^{64}\text{Ni}$  self-supporting solid target 113  $\mu\text{g}/\text{cm}^2$  thick. The  $^{16}\text{O}$  ejectiles were momentum analysed and detected at forward angles by the MAGNEX magnetic spectrometer [8], [9], [10], [11].

Exploiting the large momentum acceptance of MAGNEX (25%), energy spectra of the reaction products were obtained up to about 30 MeV excitation energy. Four angular settings were explored, with the spectrometer optical axis located at  $\theta_{opt} = 6^\circ, 12^\circ, 18^\circ$  and  $24^\circ$ , which, considering the MAGNEX solid angle (50 msr), correspond to a measured angular range  $4^\circ < \theta_{lab} < 30^\circ$ . The application of the trajectory reconstruction technique [12], [13] based on the knowledge of the 3D magnetic field maps [14], [15] and the use of the differential algebra [16], [17] did allow to get energy spectra with energy resolution of about 150 keV and angular distributions with angular resolution better than  $0.3^\circ$ .

The measured kinetic energy is shown in Fig. 1 as a function of the scattering angle for the identified  $^{16}\text{O}$  ions emitted by the  $^{64}\text{Ni}(^{18}\text{O},^{16}\text{O})^{66}\text{Ni}$  reaction. The data from four different angular settings of the spectrometer are plotted and the yields for each setting are normalized by an arbitrary scaling factor.

In the upper part of the plot one can notice the general trend of the data characterized by a kinetic energy decreasing as a function of the scattering angle. For example, the maximum kinetic energy locus, corresponding to the  $^{66}\text{Ni}$  ground state is clearly visible. This behaviour is not surprising, since it is due to the two-body kinematics.

A different trend is observed in the lower part of the plot, where the kinetic energy decreases with decreasing the angle. For these events, the initial relative motion is partially damped and a part of energy is converted from relative motion into internal degrees of freedom. This is not a kinematic effect but can be interpreted as the beginning of a more dissipative process, where the trajectories are deflected more and more from the grazing trajectory towards smaller angles and the final kinetic energy of the system decreases due to an effective nuclear friction force [18], [19].

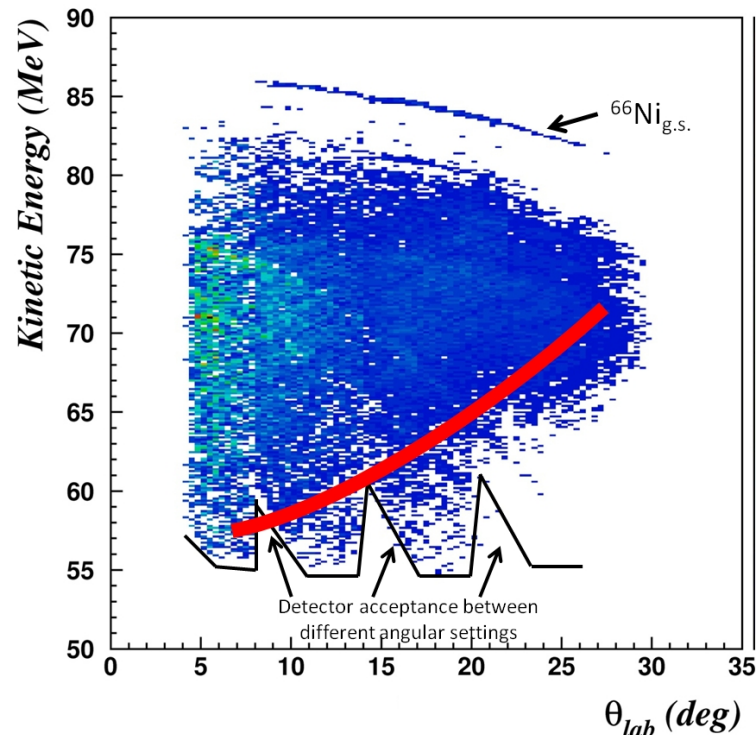


**Figure 1.** Measured kinetic energy as a function of the scattering angle for the identified  $^{16}\text{O}$  ions emitted by the  $^{64}\text{Ni}$  ( $^{18}\text{O}, ^{16}\text{O}$ )  $^{66}\text{Ni}$  reaction. Data from four different angular settings of the spectrometer at  $\theta_{opt} = 6^\circ, 12^\circ, 18^\circ$  and  $24^\circ$  are plotted and the yields for each setting are normalized by an arbitrary scaling factor. The black solid line in the lower part of the plot represents the limit of the detector acceptance. The red line is drawn just to guide the eye to show the trend of the events where the kinetic energy decreases with decreasing the angle.

### 3. Preliminary dynamical analysis

The reaction path of the ions involved in the collision was investigated in a semi-classical approach [20] by the Vlasov transport equation, where the semi-classical one-body distribution function  $f(\mathbf{r}, \mathbf{p}, t)$  follows a time evolution in the self-consistent mean-field potential  $U$ :

$$\frac{\partial f}{\partial t} + \frac{\mathbf{p}}{m} \frac{\partial f}{\partial \mathbf{r}} - \frac{\partial U}{\partial \mathbf{r}} \frac{\partial f}{\partial \mathbf{p}} = 0$$

The potential  $U$  is derived from a Skyrme-like effective interaction. Moreover, a fluctuating term is implemented in the dynamics, through stochastic spatial density fluctuations. Stochasticity is essential to get distributions, as well as to allow the growth of dynamical instabilities, see Ref. [21] for more details. In order to map the particle occupation number at each time step, Gaussian phase-space wave packets (test particles) were considered. In the performed simulations 100 test particles per nucleon were used for an accurate description of the mean field dynamics. A number of 100 events were run for each set of impact parameters.

Two typical examples of time evolution of the space density distributions projected on the reaction plane for two events of different impact parameter are shown in Fig. 2. In the more peripheral reaction (on the left side), the two fragments remain separate and a typical grazing dynamics is visible. The more central collisions (on the right side), instead, is characterized by a fusion process.

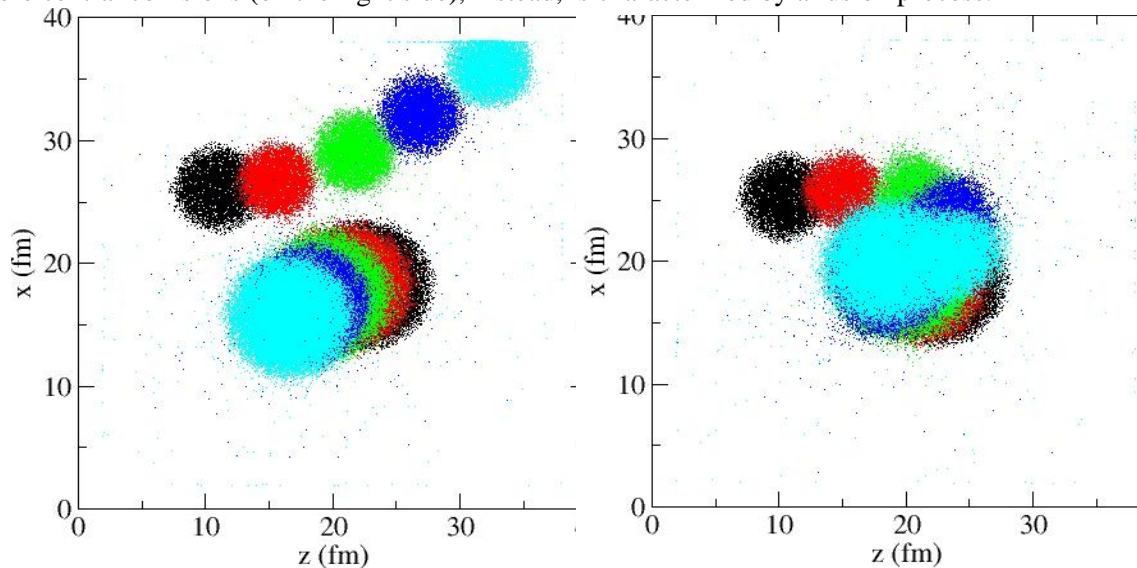


**Figure 2.** Time evolution of the space density distributions for the reaction  $^{18}\text{O} + ^{64}\text{Ni}$  at 84 MeV incident energy for impact parameter  $b = 7$  fm (left panel) and  $b = 6$  fm (right panel). The different colours represent different time steps.

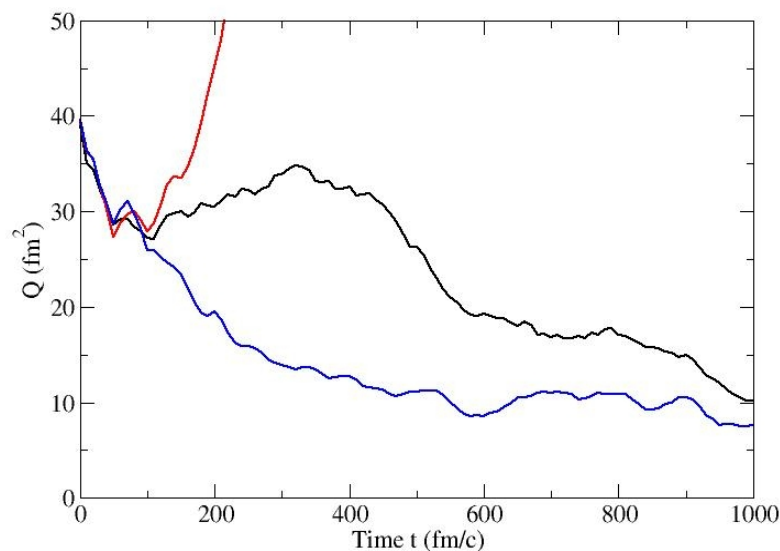


**Figure 3.** Time evolution of the space quadrupole moment for the reaction  $^{18}\text{O} + ^{64}\text{Ni}$  at 84 MeV incident energy for impact parameter  $b = 6.6$  fm. The different colours represent different events.

In the present semi-classical approach, the time evolution of the quadrupole moment in coordinate space was also extracted for each event:

$$Q(t) = \langle 2z^2(t) - x^2(t) - y^2(t) \rangle$$

where the  $z$  axis is along the rotating projectile/target direction and the  $x$  axis is on the reaction plane. In Fig. 3 the time evolution of the quadrupole moment calculated for some events of the studied reaction at the same impact parameter  $b = 6.6$  fm is plotted. The competition among different mechanisms appears. Positive values of  $Q(t)$  slope correspond to a quadrupole deformation velocity of the dinuclear system that is going to a breakup exit channel. Thus the red curve represents a typical binary process where the final system breaks in two products, while the blue curve is a fusion event. The black curve, where the quadrupole moment increases and after decreases, is an event of transition where the dynamics can evolve towards a binary process or a more dissipative one. Thus we expect to explore the conditions of kinetic energy and deflection angle observed in the data (red line in Fig.1).

#### 4. Conclusions

A preliminary analysis based on the semi-classical approach of the Vlasov transport equation was performed to describe the  $^{64}\text{Ni} (^{18}\text{O}, ^{16}\text{O}) ^{66}\text{Ni}$  reaction studied at 84 MeV incident energy by the MAGNEX spectrometer.

The time evolution of the space density distribution and of the quadrupole moment for a number of events at different impact parameters was studied. The results show that a transition from direct binary events to more dissipative processes is starting for this system in the present energy regime.

The use of the same approach to different targets excited by the same ( $^{18}\text{O}, ^{16}\text{O}$ ) reaction is planned in the near future in order to point out the systematic evolution of the reaction mechanism and establish the condition where these reactions are good spectroscopic probes.

#### 5. References

- [1] M. Cavallaro, et al., Phys. Rev. C 88, 054601 (2013).
- [2] F. Cappuzzello, et al., Phys. Lett. B 711, 347 (2012).
- [3] I. Tanihata, et al., Phys. Rev. Lett. 100, 192502 (2008).
- [4] P. D. Bond, et al., Phys. Rev. C 16, 177 (1977).
- [5] M. C. Mermaz, et al., Phys. Rev. C 20, 2130 (1979).
- [6] S. Szilner, et al., Nucl. Phys. A 779, 21 (2006).
- [7] S. Kahana and A. J. Baltz, in *Advances in Nuclear Physics*, edited by M. Baranger and E. Vogt (Plenum Press, New York, 1977), Vol. 9, pp. 1–122.
- [8] F. Cappuzzello et al., MAGNEX: an innovative large acceptance spectrometer for nuclear reaction studies in: *Magnets: Types, Uses and Safety*, Nova Publisher Inc., New York, 2011, pp 1-63.
- [9] A. Cunsolo et al., Nucl. Instrum. Methods A 484, 56 (2002).
- [10] M. Cavallaro, et al., Eur. Phys. J. A (2012) 48: 59.
- [11] F. Cappuzzello, et al., Nucl. Instr. and Meth. A 621, 419 (2010).
- [12] M. Cavallaro, et al., Nucl. Instr. and Meth. A 637, 77 (2011).
- [13] F. Cappuzzello, et al., Nucl. Instr. and Meth. A 638, 74 (2011).
- [14] A. Lazzaro, et al., Nucl. Instr. and Meth. A 585, 136 (2008).
- [15] A. Lazzaro, et al., Nucl. Instr. and Meth. A 591, 394 (2008).
- [16] K. Makino, M. Berz, Nucl. Instr. and Meth. A 427, 338 (1999).
- [17] M. Berz, K. Makino, COSY INFINITY, Version 8.1, Department of Physics and Astronomy and

- NSCL, Michigan State University, East Lansing, USA, 2001.
- [18] J. Wilczynski, Phys. Lett. B 47, 484 (1973).
  - [19] V.V. Volkov, Phys. Rep. 44, 93 (1978).
  - [20] V. Baran, et al., Phys. Rep. 410, 335 (2005).
  - [21] C. Rizzo, et al., Phys. Rev. C 83, 014604 (2011).